

Quantum Optimization for Energy Management: A Coherent Variational Approach

Farshad Amani, *Graduate Student Member, IEEE*, Amin Kargarian, *Senior Member, IEEE*

Abstract— This paper presents a quantum-enhanced optimization approach for solving optimal power flow (OPF) by integrating the interior point method (IPM) with a coherent variational quantum linear solver (CVQLS). The objective is to explore the applicability of quantum computing to power systems optimization and address the associated challenges. A comparative analysis of state-of-the-art quantum linear solvers—Harrow-Hassidim-Lloyd (HHL), variational quantum linear solver (VQLS), and CVQLS—revealed that CVQLS is most suitable for OPF due to its stability with ill-conditioned matrices, such as the Hessian in IPM. To ensure high-quality solutions, prevent suboptimal convergence, and avoid the barren plateau problem, we propose a quantum circuit parameter initialization technique along with a method to guide the IPM along the central path. Moreover, we design an ansatz tailored for OPF, optimizing the expressibility and trainability of the quantum circuit to ensure efficient convergence and robustness in solving quantum OPF. Various optimizers are also tested for quantum circuit parameter optimization, and based on the comparative analysis, the best optimizer is selected. We evaluate our approaches on IEEE 3-, 5-, 118-, and 300-bus systems, demonstrating their effectiveness in providing reliable OPF solutions. Our resource comparison between the power flow and OPF matrices on quantum hardware highlights that OPF needs considerably more resources, making its implementation significantly more challenging than in previous studies. Although promising, the application of CVQLS is currently constrained by the limitations of existing quantum hardware, especially for larger power systems. To address this, we use a quantum noise simulator for testing on larger systems.

Index Terms— Optimal Energy management, quantum linear solvers, coherent variational quantum algorithm, quantum optimization.

I. INTRODUCTION

ENERGY management is a fundamental aspect of power systems, overseeing the efficient generation, distribution, and consumption of electricity to ensure system reliability and economics. Central to this management is the challenge of optimizing the power flow (PF) within the grid, which is addressed through Optimal Power Flow (OPF). OPF focuses on optimizing electricity generation to meet demand while minimizing costs. Classical optimization methods, such as linear and nonlinear programming, have traditionally been used to solve OPF. However, these methods can struggle with scalability and computational efficiency as the complexity of power systems grows [1]–[3].

Power systems modernization, driven by technological advancements and the shift from traditional monopoly-based structures to restructured markets with multiple players and customers, has further intensified the need for faster and more efficient OPF solutions [4], [5]. While classical OPF methodologies performed adequately in simpler, traditional systems, modern power systems require optimization methods that can handle larger scales and increased complexity [6], [7]. Faster OPF solutions are crucial, particularly for short-term operational purposes such as unit commitment, $n - 1$ security, and resilience [8], [9]. Classical algorithms often exhibit cubic or polynomial computational time even in the best-case scenario [10]. Developing optimization methods that scale linearly or logarithmically with system size represents a major leap, offering the potential for exponentially faster solutions to OPF.

Several methods are used to solve OPF, ranging from classical techniques to modern optimization methods, each with varying time complexities. Classical approaches include the Newton-Raphson method, which has a computational time of $O(N^2)$ due to solving linear equations in each iteration. Despite its quadratic convergence properties, it can face convergence issues in complex systems, potentially increasing computational time [11]. Linear programming and quadratic programming methods, valued for their simplicity, generally achieve a polynomial computational time of $O(N^3)$ [12]. Machine learning approaches, such as deep learning and reinforcement learning, can reduce solution times to $O(N)$ after training, though the training phase often requires $O(N^3)$ or higher computational resources [13], [14].

IPM is highly regarded for its efficiency in handling large-scale, nonlinear constraints. It remains one of the most widely used methods for solving OPF due to its scalability, ability to handle nonlinearities, and reliable convergence. IPM solves OPF by iteratively addressing large, sparse linear systems, typically using the Newton-Raphson approach to converge toward an optimal solution [15], [16]. This iterative nature contributes to a computational time of approximately $O(N^{3.5})$, as each iteration requires solving increasingly larger systems [17]. While effective for complex and large-scale power systems, IPM's performance can be hindered by the resource-intensive need to repeatedly solve these large, often ill-conditioned linear systems, which can be nearly singular and challenging to address using classical computers.

> REPLACE THIS LINE WITH YOUR MANUSCRIPT ID NUMBER (DOUBLE-CLICK HERE TO EDIT) <

Emerging quantum computing techniques hold promise for significant advancements, potentially offering exponential speedup for OPF by leveraging advanced quantum solvers and optimization algorithms. Quantum computing presents an avenue for further improving OPF computational efficiency, despite current challenges related to noise and errors. Solving linear systems of equations is central to OPF solvers. By utilizing quantum linear solvers, we can potentially accelerate and scale power systems optimization, improving the performance of traditional methods [18]. Several quantum linear solvers have been proposed to solve linear systems more efficiently than classical methods, including Harrow-Hassidim-Lloyd (HHL) [19], variational quantum linear solver (VQLS) [20], and coherent VQLS (CVQLS) [21].

HHL offers exponential speedup over classical methods but requires fault-tolerant quantum computers, which makes it impractical for near-term, noise-sensitive devices [22], [23]. In contrast, VQLS is designed for noisy intermediate-scale quantum (NISQ) devices, using a variational approach that balances quantum and classical computations [24], [25]. The success of VQLS depends on the choice of the variational ansatz, as it influences both convergence rates and solution quality [26]. Significant research efforts have been made to optimize ansatz selection, including adaptive ansatz construction and leveraging machine learning techniques to recognize the most efficient ansatz for a given problem [26]. CVQLS further extends VQLS by incorporating coherence-preserving techniques and reducing quantum-classical interactions, which improves scalability and noise resilience [21]. Despite the potential efficiency and accuracy gains offered by CVQLS, fully realizing these benefits hinges on the availability of more advanced quantum hardware. These quantum solvers come with unique trade-offs, making them suitable for different problem scenarios and various hardware capabilities.

Applying these quantum methods as linear solvers has the potential to revolutionize multiple fields, including artificial intelligence and optimization, which are fundamental across numerous disciplines. While VQLS has found applications in areas such as machine learning [28], finite element analysis [29], and PF analysis [30], its use in solving OPF poses unique challenges. These challenges include handling sparse, ill-conditioned matrices that can require more computational resources and potentially reduce solution accuracy.

This paper addresses these challenges by exploring the application of quantum computing to OPF, focusing on the practical implementation of quantum linear solvers in power system optimization. We provide a detailed analysis of various quantum linear solvers to identify the most suitable one for our application. We formulate a quantum OPF (Q-OPF) problem and solve it using a quantum IPM (QIPM), which incorporates a CVQLS at its core. We propose several techniques to address the challenges of QIPM and improve its performance in solving Q-OPF. These include developing a tailored Q-OPF ansatz, optimizing ansatz parameter initialization to impact the search space effectively, and modifying the IPM central path to ensure

achieving high-quality solutions even in the presence of quantum computing noise and errors. Additionally, we discuss the performance of available quantum linear solver packages under real-world conditions and highlight the challenges associated with their implementation.

II. QUANTUM LINEAR SOLVERS

Solving OPF using IPM relies on solving systems of linear equations. In this context, we explore the practicality and applicability of three well-known quantum linear solvers—HHL, VQLS, and CVQLS—that can be integrated into IPM.

A. HHL

HHL is one of the seminal algorithms for solving systems of linear equations on quantum devices. It is recognized for its minimal dependency on system size and operation on a logarithmic time scale. However, the depth of the quantum circuit in HHL scales with both the size of the linear system and the condition number of matrix A (in $Ax = b$). The overall circuit depth comes from quantum phase estimation, controlled rotations, and inverse quantum Fourier transforms [31].

A significant drawback of HHL for real-world applications is its efficiency, which heavily depends on the system's condition number. As the condition number increases, the algorithm's running time also increases, making HHL potentially slower for larger matrices. Additionally, HHL is highly sensitive to noise and errors, limiting its practicality on NISQ devices. Moreover, decoding the solution from a quantum state to classical digits requires quantum tomography, which introduces a linear dependency on system size and, therefore, eliminates the logarithmic advantage of HHL.

B. VQLS

VQLS is a recently developed hybrid algorithm that addresses many of HHL limitations, albeit with a dependency on classical computers [20]. VQLS is more resilient to noise and errors, making it suitable for NISQ computers [25]. The number of qubits required to encode the state vector for a system of size N is $\log_2 N$. While the condition number influences the quantum circuit depth, the overall number of quantum gates generally increases with the complexity of the matrix and its condition. The number of cost function evaluations needed to optimize parameters in the variational ansatz also tends to rise with system size. The complexity of these evaluations is often tied to the properties of matrix A and the specific optimization algorithm used. Regarding VQLS convergence, larger, ill-conditioned systems may require more iterations to reach a solution. Sometimes, the algorithm could diverge or get stuck in a barren plateau, where progress toward the solution significantly slows or stops.

C. CVQLS

A variant of VQLS, known as CVQLS, addresses some of VQLS limitations with a tradeoff of increased classical computation to guide the quantum circuit. CVQLS reduces the overhead of quantum-classical interaction by relying more on classical computation. The performance and convergence of

> REPLACE THIS LINE WITH YOUR MANUSCRIPT ID NUMBER (DOUBLE-CLICK HERE TO EDIT) <

VQLS are strongly influenced by the choice of the variational ansatz, which defines the structure of the quantum circuit. A poor selection of ansatz can result in slow convergence or suboptimal solutions [32]. In contrast, CVQLS introduces coherence-preserving techniques that make it more resilient to quantum noise, rely less on repeated quantum measurements, have a lower circuit depth, and generally exhibit better convergence with a lower risk of encountering barren plateaus [33], [34]. These characteristics enhance CVQLS scalability and effectiveness, especially for handling ill-conditioned and large systems. By reducing the quantum-classical communication overhead, CVQLS improves efficiency regarding quantum resource utilization. Furthermore, its coherence-preserving nature leads to more accurate results with fewer quantum resources, making it a powerful tool for future quantum-augmented optimization.

D. Comparison of Quantum Linear Solvers for Q-OPF Application

Table I provides a detailed comparison of HHL, VQLS, and CVQLS. This comparison allows one to assess the strengths and weaknesses of each solver, enabling the selection of the most suitable method based on the specific requirements of the problem at hand. In the subsequent sections, we have compared the performance of VQLS and CVQLS. Based on our analysis of the advantages and disadvantages of these three quantum linear solvers, we have selected CVQLS for the Q-OPF application.

IPM in OPF often encounters ill-conditioned systems of linear equations, particularly as the algorithm progresses over multiple iterations. This worsening condition leads to increasing numerical instability, making it more difficult to solve the linear system accurately. CVQLS addresses this challenge by leveraging quantum coherence to mitigate the effects of ill-conditioning. Its ability to handle such systems more robustly makes CVQLS an ideal choice for the Q-OPF application, offering improved stability and performance as compared to other quantum solvers. CVQLS offers several key advantages that justify its selection. As demonstrated in Table I, CVQLS exhibits superior scalability compared to HHL and VQLS, making it better suited for larger and more complex systems. Additionally, CVQLS reduces the level of interaction required during the solving process, offering improved performance in noisy environments where interaction with qubits can degrade results. Finally, while both VQLS and CVQLS involve hybrid quantum-classical methods with similar computational times, CVQLS generally requires fewer iterations (T), making it more efficient in terms of execution time.

III. QUANTUM OPF

OPF is a critical problem in power systems engineering aimed at optimizing the operation of electrical power networks. The objective is to minimize the generation cost while satisfying various physical and operational constraints, including power balance, voltage limits, and generator limits. IPM is one of the most

TABLE I:
QUANTUM LINEAR SOLVERS FOR NISQ DEVICES

| | HHL | VQLS | CVQLS |
|--------------------|------------------------------------|---|---|
| Approach | Direct | Hybrid | Hybrid |
| # Qubits | $O(\log_2 N)$ | $O(\log_2 N)$ | $O(\log_2 N)$ |
| Circuit depth | $O(\text{poly}(\log_2 N, \kappa))$ | $O(\text{poly}(\log_2 N, \kappa))$ | $O(\text{poly}(\log_2 N, \kappa))$ |
| Computational time | $O(\text{poly}(\log_2 N, \kappa))$ | $O(T \times \text{poly}(\log_2 N, \kappa))$ | $O(T \times \text{poly}(\log_2 N, \kappa))$ |
| Scalability | - | + | ++ |
| Noise sensitivity | -- | ++ | ++ |
| Interaction | None | High | Reduced |
| Applicability | - | + | ++ |

T is the number of iterations, and $T_{CVQLS} \leq T_{VQLS}$.

popular and effective methods for solving OPF, iteratively refining the solution by solving a series of linear equations [35]. We integrate CVQLS into IPM to solve the linear system of equations encountered at each iteration to determine the Newton direction.

A. OPF Formulation

A compact OPF formulation is as follows [36]:

$$\min_{P_G, Q_G} f(P_G, Q_G)$$

subject to:

$$\begin{aligned} P_G - P_D &= BV, \\ Q_G - Q_D &= GV, \\ V_{\min} &\leq V \leq V_{\max}, \\ P_{G,\min} &\leq P_G \leq P_{G,\max}, \\ Q_{G,\min} &\leq Q_G \leq Q_{G,\max}, \end{aligned} \quad (1)$$

where P_G and Q_G are active and reactive power generations, P_D and Q_D are active and reactive power demands, V represents bus voltages, and B and G are the admittance matrices.

B. Interior Point Method

IPM solves OPF by iteratively finding the Newton direction through a series of transformations and optimizations. We briefly overview the steps involved in IPM and then explain how they can be adapted to a QIPM.

Step 1: Converting Inequalities into Equalities: Inequality constraints are converted into equality constraints using slack variables. For example, the voltage constraints $V_{\min} \leq V \leq V_{\max}$ are transformed as:

$$\begin{aligned} V - s_1 &= V_{\min}, \\ V + s_2 &= V_{\max}, \end{aligned} \quad (2)$$

where s_1 and s_2 are slack variables ensuring non-negativity.

Step 2: Non-negativity as a Logarithmic Barrier: Non-negativity constraints on the slack variables are penalized in the objective function using a logarithmic barrier function.

$$\Phi(x, \mu) = f(P_G, Q_G) - \mu \sum_i \ln(s_i), \quad (3)$$

where μ is a positive parameter that controls the barrier's influence.

Step 3: Forming an Unconstrained Optimization Function: An unconstrained optimization problem is formulated as a Lagrangian function, which incorporates both modified objective function and equality constraints:

> REPLACE THIS LINE WITH YOUR MANUSCRIPT ID NUMBER (DOUBLE-CLICK HERE TO EDIT) <

$$\begin{aligned} \mathcal{L}(x, \lambda, \nu) = & \Phi(x, \mu) + \sum_j \lambda_j (h_j(x) - b_j) \\ & + \sum_k \nu_k (g_k(x) - c_k) \end{aligned} \quad (4)$$

where λ and ν are Lagrange multipliers for the equality and inequality constraints, respectively.

Step 4: Newton Direction Matrix: The Newton direction Δx is obtained by solving perturbed Karush-Kuhn-Tucker (KKT) conditions, which require solving a linear system of equations. To reduce the size of the Newton matrix, we exploit the sparsity of the Hessian H_k and the Jacobian matrices and use matrix factorization techniques. The reduced KKT system is:

$$\begin{bmatrix} H_k & J_k^T \\ J_k & 0 \end{bmatrix} \begin{bmatrix} \Delta x \\ \Delta \lambda \end{bmatrix} = - \begin{bmatrix} r_k \\ c_k \end{bmatrix}, \quad (5)$$

where H_k is the Hessian matrix, J_k is the Jacobian matrix, r_k is the residual vector, and c_k is the constraint vector. The smaller reduced system of equations maintains the essential structure for finding the Newton direction while minimizing computational complexity.

The next section explains the use of CVQLS as the quantum linear solver to determine the Newton direction Δx .

C. CVQLS for Newton Direction

Building on CVQLS advantages, we use it as the quantum linear solver to determine the Newton direction. By leveraging the coherence-preserving capabilities of CVQLS, we can improve the efficiency and accuracy of solving linear systems required to determine the Newton direction.

To solve the linear system $H_k \Delta x_k = -r_k$ using CVQLS, it is necessary to represent the Hessian matrix H_k in a quantum state. Several methods exist for encoding classical matrices into quantum states or decomposing them into unitary operators. Each method has distinct characteristics, advantages, and limitations depending on the nature of the matrix and the specific quantum algorithm being applied. Table II provides an overview of some common encoding methods [37]–[41].

TABLE II:

COMPARISON OF QUANTUM MATRIX ENCODING METHODS

| | # Qubits | Complexity | Matrix Type | Limitation |
|-----------------------|----------|------------|-------------|-------------------------|
| Basic encoding | ++ | -- | Arbitrary | High # qubits |
| Amplitude encoding | - | + | Normalized | Arbitrary data |
| Qubitization | + | +++ | Sparse | High complexity |
| Matrix exponentiation | + | ++ | Hermitian | Resource intensive |
| Pauli decomposition | + | + | Hermitian | Scales with matrix size |

Among these encoding methods, we chose Pauli decomposition to encode the classical matrix. Pauli matrices form a complete basis for Hermitian matrices, making them particularly suitable for quantum algorithms that operate on Hermitian operators, like CVQLS. The decomposition of a Hermitian matrix into a linear combination of Pauli matrices allows the representation of the matrix in a form that is naturally compatible with quantum circuits. Furthermore, the scalability of Pauli decomposition through tensor products of Pauli matrices enables the efficient representation of larger matrices, such as those encountered in OPF. This approach simplifies the

translation of classical matrix operations into quantum gates, making it an ideal choice for Q-OPF.

We decompose the Hermitian matrix ($H_k^\dagger = H_k$) into a combination of four Pauli matrices as follows:

$$I = \begin{pmatrix} 1 & 0 \\ 0 & 1 \end{pmatrix}, \quad X = \begin{pmatrix} 0 & 1 \\ 1 & 0 \end{pmatrix}, \quad Y = \begin{pmatrix} 0 & -i \\ i & 0 \end{pmatrix}, \quad Z = \begin{pmatrix} 1 & 0 \\ 0 & -1 \end{pmatrix} \quad (6)$$

Assume we have a random Hermitian matrix $H_k = \begin{pmatrix} H_k^{11} & H_k^{12} \\ H_k^{21} & H_k^{22} \end{pmatrix}$. We form a linear combination of Pauli matrices as follows [40]:

$$\begin{aligned} \beta_0 I + \beta_1 X + \beta_2 Z + \beta_3 Y &= \begin{pmatrix} \beta_0 + \beta_2 & \beta_1 - i\beta_3 \\ \beta_1 + i\beta_3 & \beta_0 - \beta_2 \end{pmatrix} \\ &= \begin{pmatrix} H_k^{11} & H_k^{12} \\ H_k^{21} & H_k^{22} \end{pmatrix} \end{aligned} \quad (7)$$

Given a matrix H_k , coefficients β_i can be determined. For larger matrices, the combination of tensor products of Pauli matrices can be used to represent H_k . For a 4×4 matrix, the combination are:

$$\begin{aligned} \beta'_0 (I \otimes I) + \beta'_1 (I \otimes X) + \beta'_2 (I \otimes Y) + \beta'_3 (I \otimes Z) \\ + \beta'_4 (X \otimes I) + \dots + \beta'_{15} (Z \otimes Z) \end{aligned} \quad (8)$$

where \otimes denotes the tensor product, and the coefficients β'_i correspond to the contribution of each Pauli matrix combination in the representation of H_k .

Consider a matrix H_k of size $2^n \times 2^n$, that is expressed as a linear combination of L unitary matrices $H_{k_0}, H_{k_1}, \dots, H_{k_{L-1}}$. Each of these unitary matrices, H_{k_l} , must be efficiently implemented through a quantum circuit that acts on n qubits. The coefficients α_l in this linear combination, represented in equation (9), are part of a normalized and positive probability distribution. The complex phase of each coefficient α_l can be absorbed into the corresponding unitary matrix H_{k_l} , leaving us with a vector of positive values for α_l .

$$\alpha_l \geq 0 \quad \forall l, \quad \sum_{l=0}^{L-1} \alpha_l = 1. \quad (9)$$

where $L = 2^m$ and m is a positive integer. This normalization ensures that α_l forms a probability distribution, as the linear problem is defined up to a scaling factor.

Next, we introduce a unitary circuit U_α that embeds the square root of α into the quantum state $|\sqrt{\alpha}\rangle$ on m ancillary qubits as:

$$|\sqrt{\alpha}\rangle = U_\alpha |0\rangle = \sum_{l=0}^{L-1} \sqrt{\alpha_l} |l\rangle, \quad (10)$$

Where $|l\rangle$ denotes the computational basis state of the ancillary qubits.

For each unitary matrix H_{k_l} , we define a controlled unitary operation $C_{H_{k_l}}$ that acts on both the system and the ancillary qubits. The controlled unitary applies H_{k_l} only when the ancillary qubits are in the corresponding basis state $|l\rangle$. This operation can be described as:

> REPLACE THIS LINE WITH YOUR MANUSCRIPT ID NUMBER (DOUBLE-CLICK HERE TO EDIT) <

$$C_{H_{k_l}}|j\rangle|l'\rangle = \begin{cases} (H_{k_l} \otimes I)|j\rangle|l\rangle & \text{for } l' = l, \\ |j\rangle|l'\rangle & \text{for } l' \neq l, \end{cases} \quad (11)$$

In this case, the unitary H_{k_l} is applied to the system qubits when the ancillary qubits are in the state $|l\rangle$, while the state remains unchanged if the ancillary qubits are in any other basis state. This construction allows for the selective application of the unitaries in the linear combination based on the state of the ancillary system.

CVQLS approximates the solution $|\Delta x_k\rangle$ with a variational quantum circuit $V(\omega)$:

$$|\Delta x_k\rangle = V(\omega)|0\rangle, \quad (12)$$

The given complex vector $-r_k$ must be generated by a unitary operation U_{r_k} applied to the ground state of n qubits to have the quantum state $|r_k\rangle$:

$$|-r_k\rangle = U_{r_k}|0\rangle, \quad (13)$$

To solve $H_k \Delta x_k = -r_k$ we prepare a quantum state $|\Delta x_k\rangle$ such that $H_k |\Delta x_k\rangle$ is proportional to $|-r_k\rangle$, i.e.,

$$|\Psi\rangle := \frac{H_k |\Delta x_k\rangle}{\sqrt{\langle \Delta x_k | H_k^\dagger H_k | \Delta x_k \rangle}} \approx |-r_k\rangle. \quad (14)$$

where ω are the variational parameters. The cost function to be minimized is:

$$C_{\text{coherent}} = 1 - |\langle -r_k | \Psi_k \rangle|^2 + \lambda_k \mathcal{C}(V(\omega_k)) \quad (15)$$

$\mathcal{C}(V(\omega_k))$ is a coherence measure of the variational circuit, and λ_k is a regularization parameter of k^{th} iteration. Minimizing C_{coherent} with respect to ω yields the optimal parameters for the variational circuit.

The pseudo-code of solving OPF using CVQLS is shown in Algorithm I. This integrated approach combines the robustness of IPM with the computational power of quantum algorithms through CVQLS, with quantum circuits solving the linear systems and classical computations handling the parameter tuning and overall optimization process. The process is illustrated in Fig. 1, in which all classical computations are shown on the right side within a dashed box, while the left side demonstrates the Newton step solution utilizing CVQLS. This is a hybrid approach where the optimization process involves quantum circuit parameter tuning managed by a classical computer. Each IPM iteration needs corresponding iterations of CVQLS to solve the linear equations.

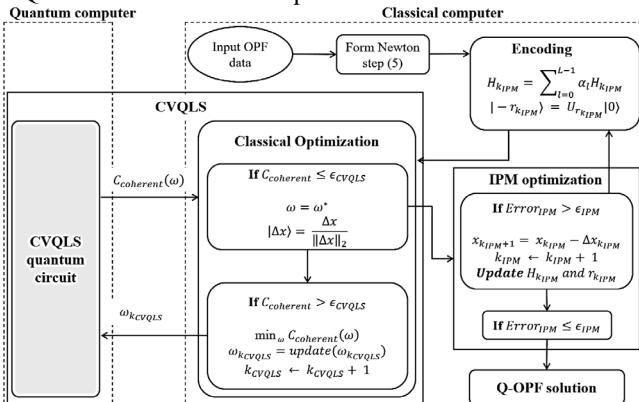


Fig. 1: The hybrid approach of solving OPF using CVQLS.

Algorithm I: Q-OPF Using CVQLS

- 1: **Input:** OPF data
 - 2: Form unconstrained OPF optimization (4)
 - 3: Form system of linear equation (5) to find $H_{k_{IPM}} \Delta x_k = -r_k$
 - 4: **While:** $\epsilon_{IPM} < \epsilon_0$ or $k_{IPM} < k_{IPM}^{max}$
 - 5: Initialize $x_{k_{IPM}}$ to find classical values
 - 6: Encode $H_{k_{IPM}}$ and $-r_{k_{IPM}}$ into quantum state
 - 7: Prepare all qubits in the ground state
 - 8: Apply U_α to ancillary qubits
 - 9: Apply the variational circuit V to linear system of equation
 - 10: Apply all controlled unitaries $C_{H_{k_{IPM}l}}$ for all l
 - 11: Apply U_α^\dagger to ancillary qubits
 - 12: Measure ancillary qubits on a computational basis:

$$|\Psi_{k_{IPM}}\rangle := \frac{H_{k_{IPM}} |\Delta x_{k_{IPM}}\rangle}{\sqrt{\langle \Delta x_{k_{IPM}} | H_{k_{IPM}}^\dagger H_{k_{IPM}} | \Delta x_{k_{IPM}} \rangle}}$$
 - 13: Apply $U_{r_{k_{IPM}}}^\dagger$ to linear system of equation
 - 14: Measure system of equation to find (14) or probability of equations in the ground state
 - 15: Form a modified cost function (15)
 - 16: **while** $C_{\text{coherent}} < \epsilon_{CVQLS}$ and $k_{CVQLS} < k_{CVQLS}^{max}$
 - 17: Optimize variational parameters $\omega_{k_{CVQLS}}$ of cost function to minimize C_{coherent} to find $\Delta x_{k_{IPM}}$
 - 18: **end**
 - 19: $x_{k_{IPM}+1} = x_{k_{IPM}} - \Delta x_{k_{IPM}}$
 - 20: $k_{IPM} \leftarrow k_{IPM} + 1$
 - 21: Calculate ϵ_{IPM}
 - 22: **end**
- Return:** The solution of Q-OPF
-

IV. PROPOSED Q-OPF IMPROVEMENT TECHNIQUES

The current commercial quantum linear solvers are primarily designed for proof-of-concept purposes and work under controlled conditions. Significant adjustments are required for practical, real-world applications due to the substantial impact of the problem's physics on various aspects of algorithms. Since we opted for the variational method, we will first outline the key components of these algorithms and techniques used to optimize their performance for our specific application, OPF. Subsequently, we will also examine necessary adjustments for the QIPM calculations.

A. Variational Quantum Optimization Landscape

In variation quantum algorithms, the quantum circuit parameter optimization landscape is influenced by the choice of the variational ansatz and its parameter initialization. These factors determine whether the optimization process encounters barren plateaus or converges to a solution.

Fig. 2 illustrates different optimization landscapes encountered in CVQLS [42], [43]. In Fig. 2(a), no barren plateau is observed, as multiple viable paths lead to the solution. This occurs when the ansatz is well-structured, and parameter initialization is near the optimal region, facilitating smooth convergence. Fig. 2(b) shows an optimization landscape approaching a barren plateau, where several local minima exist, and only a few paths guide the optimization towards the global minimum. Such a landscape can arise when the ansatz is moderately complex or when parameter initialization is less favorable, limiting the number of successful optimization routes. Fig. 2(c) shows a nearly barren plateau with few paths to the solution. The flat landscape indicates an overly complex or poorly chosen ansatz, resulting in limited convergence

> REPLACE THIS LINE WITH YOUR MANUSCRIPT ID NUMBER (DOUBLE-CLICK HERE TO EDIT) <

regions. This often occurs in CVQLS due to inefficient optimization, such as over-parameterization or poor initialization.

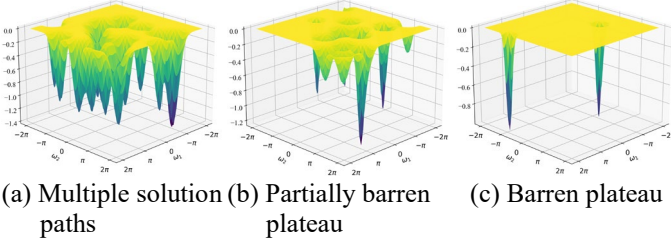


Fig. 2: Variational quantum optimization landscape with different settings.

B. OPF-Tailored Ansatz

The choice of ansatz is crucial for CVQLS performance. The ansatz is shallow or deep, presenting distinct characteristics and trade-offs. The depth variable controls the number of layers in the ansatz, where each layer typically consists of Ry gates (rotation around the Y-axis) followed by CZ gates (controlled-Z gate). Ry gate performs a rotation of the qubit's state around the Y-axis on the Bloch sphere. It takes a parameter ϕ and transforms the qubit state based on that angle. In the ansatz, Ry gates allow for continuous tuning of the qubit states to optimize the solution. CZ gate is a two-qubit gate that applies a Z-phase flip (changes the phase of the qubit state) on the second qubit if the first qubit is in the $|1\rangle$ state. In the ansatz, CZ gates create entanglement between qubits, enabling complex interactions to solve linear systems.

Depending on the problem, selecting an appropriate ansatz is important for CVQLS [44]. A shallow ansatz reduces the expressivity of the quantum circuit, making it less capable of representing complex functions. Consequently, to accurately approximate the solution of the linear system, a deeper ansatz with higher expressivity might be necessary. However, increasing the depth of the ansatz can introduce trainability challenges. A more complex circuit complicates the optimization landscape, increasing the likelihood of encountering barren plateaus where the cost function gradient is nearly zero. Furthermore, while a deeper ansatz can lead to overfitting, a shallow ansatz might fail to find the solution, resulting in poor convergence [24], [45], [46]. The comparison of a shallow and deep ansatz is given in Table III.

TABLE III:

| ANSATZ EFFECTS | | |
|----------------|------------|----------------------|
| | Shallow | Deep |
| Expressivity | Limited | High |
| Trainability | Easy | Hard |
| Overfitting | Low risk | High risk |
| Convergence | Fast | Slow |
| Optimization | Fast | Slow |
| Noise | Less prone | Susceptible to noise |

We used two ansatzes shown in Fig. 3. Based on our observations, the shallow ansatz Fig. 3(a) shows stable and reliable convergence in our study. However, the deeper ansatz shown in Fig. 3(b) either converges very slowly or fails to reduce CVQLS cost function effectively. Thus, we suggest the shallow ansatz for the Q-OPF application.

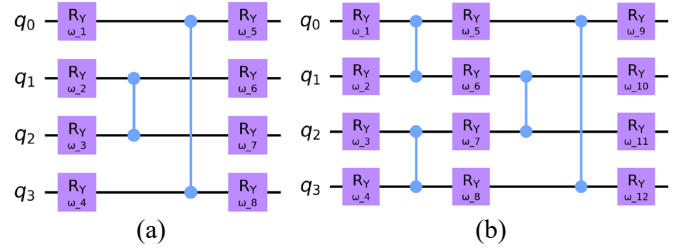


Fig. 3: a) Shallow, and b) deep ansatzes.

C. CVQLS Parameter Initialization

Proper initialization of ansatz parameters is crucial for CVQLS performance, as these initial values significantly influence the optimization landscape the algorithm explores. Poor initialization might place the optimization process in regions of the landscape where the cost function is flat, known as barren plateaus, leading to slow or stalled convergence. In contrast, a well-chosen initialization can position the algorithm closer to a good solution, enhancing convergence speed and reducing the number of iterations between classical and quantum computing devices.

Avoiding local minima is another important role that good initialization plays. A more informed initialization can provide a better starting point, making it easier to reach the global minimum. The challenge of barren plateaus, where the cost function gradient is nearly zero over large regions of the parameter space, is a significant concern in variational quantum algorithms like CVQLS. Proper parameter initialization can help mitigate this issue by starting the optimization in a region where the gradients are not flat, making it easier to find a descent direction [34], [46]. We used two different methods for the initialization:

Fixed Value Initialization: Initially, we tested the default parameter initialization provided by the PennyLane CVQLS package, where all parameters are set to a fixed value of one. This method, though simple, led to unsatisfactory outcomes. The fixed initialization resulted in high errors and unstable convergence. In many cases, the quantum circuit parameter optimization process did not converge, leading to CVQS divergence. These issues are likely due to the limited exploration of the parameter space. The algorithm struggled to adjust the parameters effectively, often stuck in local minima and failing to find a viable path toward the optimal solution.

Sequential Initialization Using Parameters from Previous Iterations: The second approach involved using the parameters obtained from the final iteration of the previous CVQLS run as the initial parameters for the subsequent OPF iteration. Since the structure of the matrices H_K and H_{K+1} in successive OPF iterations is similar, this method leverages the proximity of these solutions in the parameter space. Given that the structure of the H matrices is close between iterations, this approach works well, allowing the optimization to start from a more informed position and reducing the number of iterations needed to reach a solution. While the fixed value initialization was the least effective, the sequential initialization based on prior knowledge yielded significantly better results. Hence, we suggest using the second method.

D. Quantum Circuit Parameter Optimization Methods

Optimization methods are crucial for minimizing the CVQLS cost function and tuning circuit parameters. These methods are

> REPLACE THIS LINE WITH YOUR MANUSCRIPT ID NUMBER (DOUBLE-CLICK HERE TO EDIT) <

categorized as gradient-based, quasi-Newton, and non-gradient-based optimization approaches [20], [25], [47].

Quasi-Newton methods approximate second-order information (the Hessian) to update parameters. These methods can converge faster than basic gradient descent but are computationally more expensive, especially for high-dimensional problems. In the context of CVQLS, the Broyden–Fletcher–Goldfarb–Shanno (BFGS) algorithm works well for small quantum systems but becomes impractical for larger, more complex ones due to its reliance on second-order approximations.

Non-gradient-based optimizers do not require gradients and use linear approximations to optimize the cost function. This makes COBYLA a robust option for quantum systems where gradients are noisy or difficult to compute. However, it tends to converge more slowly compared to gradient-based methods. COBYLA is suitable for noisy quantum environments, making it particularly useful in some cases of CVQLS, especially when working on near-term quantum hardware.

Gradient-based optimizers rely on the computation of gradients to guide parameter updates. Adam, in particular, adapts the learning rate for each parameter based on first and second-moment estimates, making it efficient for large-scale optimization problems. Based on our observations explained in the case study section, we suggest Adam as a preferred choice for CVQLS due to its ability to handle large parameter spaces and accelerate convergence. Table IV provides a comparison between the three quantum circuitry optimizers.

TABLE IV:

| QUANTUM CIRCUIT PARAMETER OPTIMIZATION METHODS | | | |
|--|--------------------------|----------------------------|----------------------|
| | Gradient-based | Quasi-Newton | Non-gradient-based |
| Example | Adam | BFGS | COBYLA |
| Gradient Requirement | Yes | Yes (Hessian approx.) | No |
| Computation Efficiency | High (adaptive learning) | Medium (second-order info) | Low (linear approx.) |
| Convergence Speed | Fast | Medium | Slow |
| Applicability | VQLS and CVQLS | Small systems | Noisy systems |

E. QIPM Central Path Direction

Controlling the IPM convergence is another crucial factor, particularly because Newton's direction might be erroneous due to quantum noise and error. A key parameter in IPM for finding the optimal solution is μ , which balances the tradeoff between optimality and feasibility. The parameter μ is linked to the barrier term in IPM's objective function, which penalizes proximity to the boundaries of the feasible region. Effectively managing μ ensures that the iterates stay within the interior of the feasible region, contributing to numerical stability and preventing issues such as ill-conditioning that could occur if the iterates get too close to the boundary.

μ , also, helps guide the iterates along the central path—a trajectory through the interior of the feasible region that IPM follows toward the optimal solution. The central path acts as a buffer, keeping the iterates away from the boundary, where numerical instability and ill-conditioning are more likely to occur. By controlling μ , we ensure that the iterates stay

sufficiently close to this central path, preventing divergence or instability as the solution progresses.

Choosing $\mu \approx 0$ emphasizes finding the optimal solution by rapidly tightening the complementary gap, while a larger μ ensures the feasibility of the solution. Generally, a slower decrease in μ may result in more iterations but provides greater stability. Conversely, a more aggressive decrease can speed up convergence but risks instability or divergence if the updates are too large [48], [49].

Various methods and formulations have been introduced to update μ during IPM iterations. Since we are working with an inexact linear solver in this study, we retain the original formulation of MatPower's IPM but with some modifications [15], [49].

Our experiments revealed that classical IPM methods tend to reduce μ too quickly. When using an inexact linear solver, more IPM iterations are needed to reach a solution, so we must carefully control the reduction rate of μ . If μ is set too small in the early iterations, the central path tightens quickly. It approaches the boundary of the feasible region, potentially leading to a local optimum or incorrect solution.

To address this, we monitor IPM objective function value across iterations. Specifically, we compute the average of IPM objective function values over n consecutive iterations using (16).

$$\text{avg}_k = \frac{1}{n} \sum_{i=k-n}^{k-1} f_i \quad \forall k = n+1, n+2, \dots, k^{\max} \quad (16)$$

(16) allows us to smooth changes in IPM objective function and detect any trends in its behavior. To determine whether IPM objective function values are stabilizing, we compute the relative difference between the average value and the next iteration's objective value, as defined by (17).

$$\text{relDif}_k = \left| \frac{\text{avg}_k - f_{k+1}}{\text{avg}_k} \right| \quad \forall k = n+1, n+2, \dots, k^{\max} \quad (17)$$

By monitoring relDif_k , we can dynamically control μ updates based on the behavior of IPM objective function. If relDif_k falls below a threshold, or if the IPM objective function exhibits a sudden deviation beyond $\pm 20\%$ of avg_i over the last few iterations, we fix μ to ensure stability. Otherwise, μ is updated dynamically according to classical IPM. This approach ensures that μ remains stable during periods of large fluctuations while adapting when convergence is steady. Typically, μ is only fixed once in the early stages of the OPF iteration to let the solver find the correct central path to the optimal solution. This process is further detailed in Algorithm II, and visual representations are in Fig. 4.

Algorithm II: μ correction for guiding QIPM central path

Input: Objective function of QIPM

1: **While** $k < k^{\max}$

2: Run QIPM and store the objective function

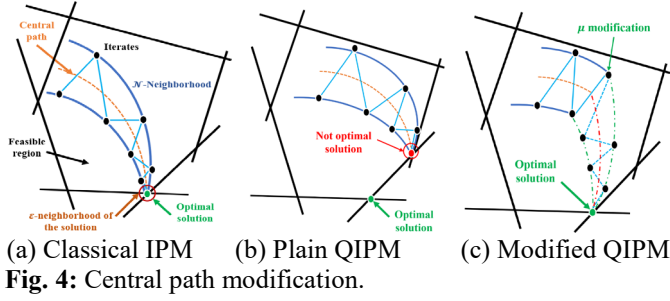
3: **If** $\text{relDif}_k < \epsilon_{\text{conv}}$ **or** $f_k < 0.8 \times \text{avg}_i$ **or** $f_k > 1.2 \times \text{avg}_i$
 fix the value of μ to be the same as iteration number k
 $k \leftarrow k + 1$

4: **Elseif** $\text{relDif}_k > \epsilon_{\text{conv}}$ **or** $0.8 \times \text{avg}_i < f_k < 1.2 \times \text{avg}_i$
 update μ
 $k \leftarrow k + 1$

5: **End**

Return: Value of μ

> REPLACE THIS LINE WITH YOUR MANUSCRIPT ID NUMBER (DOUBLE-CLICK HERE TO EDIT) <



V. CASE STUDY

A. Simulation Setting

To evaluate the proposed approaches, we tested them on two small systems (3-bus and 5-bus) and two larger systems (118-bus and 300-bus). CVQLS simulations are conducted using the PennyLane package with Python on a PC with 16 GB of RAM. Adam, BFGS, and COBYLA are used to optimize VQLS and CVQLS quantum circuit parameters. As shown in Table VI, encoding for large systems such as the 118-bus and 300-bus encountered out-of-memory errors. Additionally, due to the substantial size of the Hessian matrix in these systems, simulating quantum computers on classical hardware is both inefficient and challenging. Therefore, while CVQLS was simulated for the small systems, for the larger systems, we modeled quantum errors and noise using the Qiskit noise simulator and incorporated these into the computations. For OPF simulation with IPM method, MatPower 8.0 is used.

B. OPF vs. PF

Solving linear systems of equations is a key component in both PF and OPF studies. The condition numbers of PF matrices are smaller than those of OPF matrices. Table V presents the condition numbers for PF and OPF problems, highlighting the ill-conditioned nature of OPF matrices compared to those in PF studies. A poorly conditioned matrix complicates the encoding process of matrix H_k , leading to higher computational costs and increased susceptibility to noise and errors in calculations. For instance, encoding the first iteration of DCOPF in a 3-bus system needs a circuit with 364 gates:

$$\begin{aligned}
 & 3771.0073 \cdot IIII + 3494.7806 \cdot ZIZI - 3282.7582 \cdot IIZZ + \\
 & \quad \dots + (85 \text{ other terms}) + \dots \\
 & + 0.3405 \cdot ZXXX - 0.0931 \cdot ZZZX - 0.0139 \cdot ZYYY
 \end{aligned} \tag{18}$$

In contrast, encoding the 3-bus system PF matrix requires three gates.

$$2.6953 \cdot I - 1.3333 \cdot X - 0.2509 \cdot Z \tag{19}$$

The number of controlled Pauli gates for encoding the Hessian matrix (H_k) in the last iteration of Newton's step for different systems are displayed in Table VI. In addition, the matrix size in OPF is larger than that of PF, worsening the situation. Table VII shows the sizes of matrices for different systems. These factors make solving OPF with QIPM more complex than solving PF, emphasizing the need for carefully designed and sophisticated approaches to address OPF in a quantum computing setting.

TABLE V:
CONDITION NUMBERS OF PF AND OPF

| | DCPF | ACPF | | DCOPF | | ACOPF | |
|---------|-------|-------|-------|-------|------|-------|------|
| | | min | max | min | max | min | max |
| 3-bus | 3.3 | 3.03 | 4.65 | 1.9e4 | 3e17 | 41 | 1e11 |
| 5-bus | 11.4 | 16.1 | 16.2 | 1.1e4 | 7e19 | 2.2e4 | 3e11 |
| 118-bus | 1.7e4 | 3.1e3 | 3.1e3 | 3e7 | 2e14 | 6.7e3 | 2e9 |
| 300-bus | 1.3e5 | 1.1e5 | 1.1e5 | 4e7 | 5e7 | 1e6 | 3e12 |

TABLE VI:
REQUIRED RESOURCES FOR ENCODING HK

| | 3-bus | 5-bus | 118-bus | 300-bus |
|-------|-------|-------|---------|---------|
| DCPF | 18 | 62 | Error | Error |
| DCOPF | 364 | 308 | Error | Error |
| ACPF | 3 | 70 | Error | Error |
| ACOPF | 1548 | 1840 | Error | Error |

TABLE VII:
MATRIX SIZE

| | DCPF | ACPF | DCOPF | ACOPF |
|---------|------|------|-------|-------|
| 3-bus | 3 | 2 | 10 | 19 |
| 5-bus | 5 | 5 | 16 | 31 |
| 118-bus | 118 | 181 | 291 | 581 |
| 300-bus | 300 | 530 | 670 | 1339 |

C. CVQLS vs. VQLS

We have tested Adam and COBYLA optimizers to solve the 16x16 matrix in the 3-bus system during the third iteration of QIPM using VQLS. Although, according to Table IV, Adam is expected to perform the best, as shown in Fig. 7(a), it did not yield satisfactory results and became stuck in a barren plateau situation. COBYLA is applied to the same matrix and demonstrated better results, as illustrated in Fig. 5. However, COBYLA exhibits very slow convergence and the number of quantum-classical iterations varies even when the model is rerun under identical conditions. Fig. 5 illustrates the convergence behavior of VQLS. While the solution approaches the target, fluctuations occur throughout the convergence process. Fig. 5(b) indicates that additional iterations are needed when rerunning the simulation with the same matrix. Also, the solution error is higher in the first case. This suggests that although VQLS performs effectively, achieving consistent results for larger systems can be challenging.

For larger matrices like 32x32 in the 5-bus system during the second QIPM iteration, we had even more challenges. We observed that the computational costs of VQLS to solve the equation $H_k \Delta x_k = -r_k$, increases as the system size grows. However, to find a better behavior, one can change the ansatz and VQLS optimizer and use different ansatz initializations. For example, we have obtained acceptable results for a 32x32 matrix in the second iteration of ACOPF for the 5-bus system using padding to make the matrix Hermitian and the BFGS optimizer. However, this came with trade-offs: the optimization process was time-consuming and exhibited oscillatory behavior in the cost function, as shown in Fig. 6. As shown in Fig. 7(b), we have observed that the COBYLA optimizer encounters a barren plateau situation after a time-consuming process and is unable to find the optimal solution.

> REPLACE THIS LINE WITH YOUR MANUSCRIPT ID NUMBER (DOUBLE-CLICK HERE TO EDIT) <

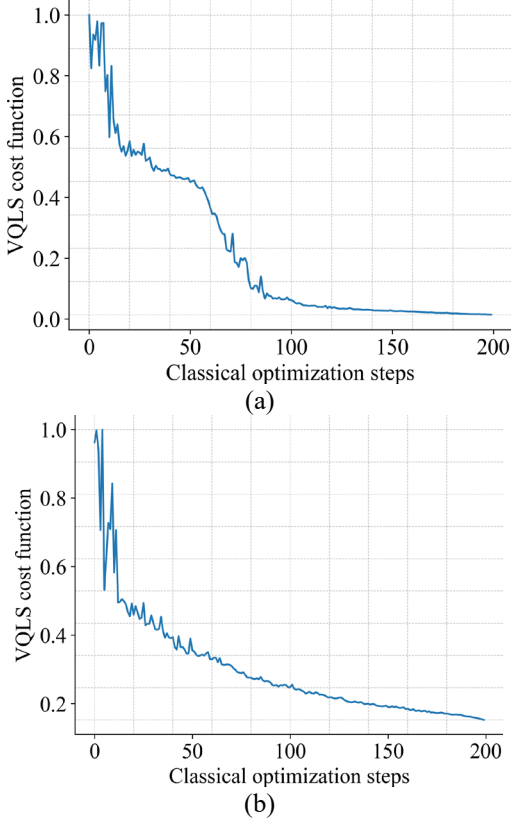


Fig. 5: VQLS cost function of the third QIPM iteration for DCOPF in 3-bus system: (a) first run, and (b) second run.

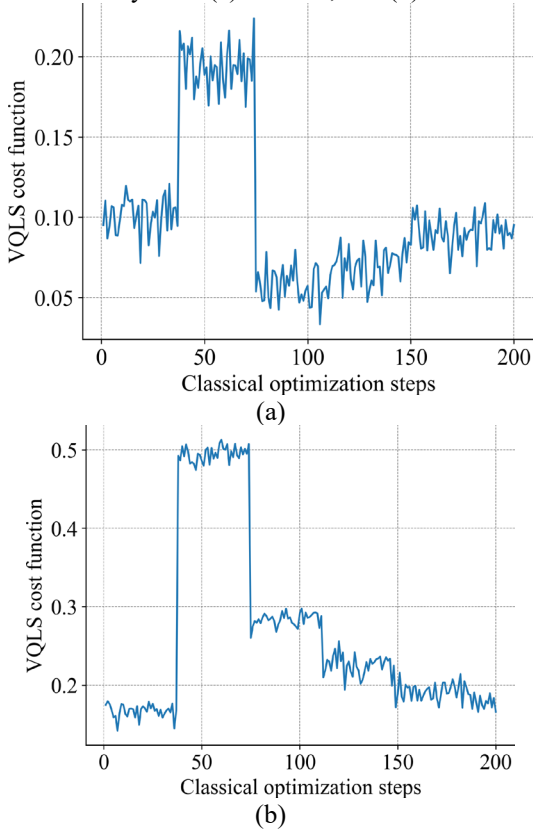


Fig. 6: VQLS cost function of the second QIPM iteration for ACOPF in 5-bus system: (a) first run, and (b) second run.

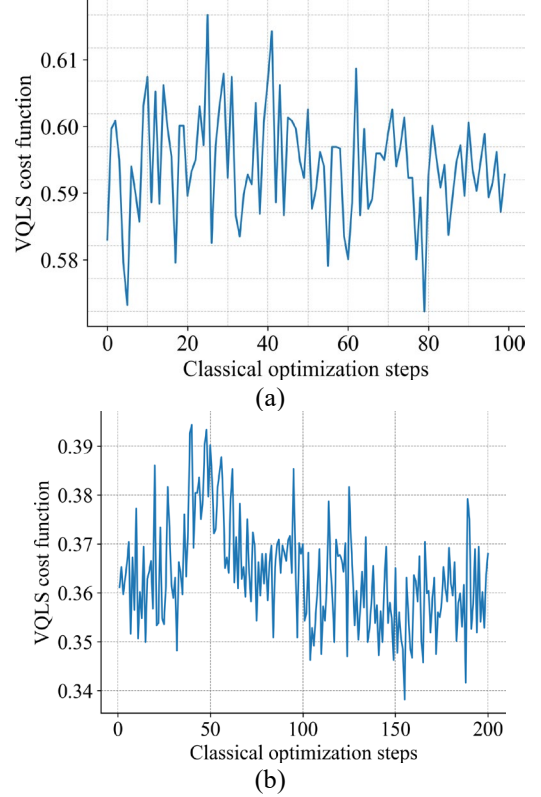


Fig. 7: VQLS cost function (a) in the third iteration of 3-bus system using Adam and (b) in the second iteration of 5-bus system using COBYLA.

These observations highlight the limitations of VQLS in solving OPF matrix equations with high accuracy. The time-consuming nature of the computation and the variability in error underscore the need for further refinement in quantum algorithms to enhance their reliability and efficiency for such applications. This extended computation time poses substantial difficulties in efficiently solving ACOPF.

We have explored CVQLS capabilities to address these issues. CVQLS offers several advantages over VQLS, including improved convergence properties and reduced computational overhead. By leveraging coherent quantum operations and optimized variational approaches, CVQLS can potentially enhance the efficiency and accuracy of solving complex optimization problems. This approach aims to address the computational difficulties observed with VQLS and improve the overall feasibility of finding solutions to OPF, particularly for ACOPF. For instance, in the case of 8×8 and 16×16 matrices, the convergence behavior observed is illustrated in Fig. 8. For a larger matrix with a size of 32×32 , CVQLS performance is shown in Fig. 9. As Fig. 9, the quantum circuit cost function smoothly decreases towards lower values with consistently small errors, even when the same matrix is run multiple times. These improvements in both convergence stability and computational efficiency suggest adopting CVQLS for the Q-OPF application. Note that for CVQLS, we have exclusively used the Adam optimizer and did not encounter the challenges observed in VQLS.

> REPLACE THIS LINE WITH YOUR MANUSCRIPT ID NUMBER (DOUBLE-CLICK HERE TO EDIT) <

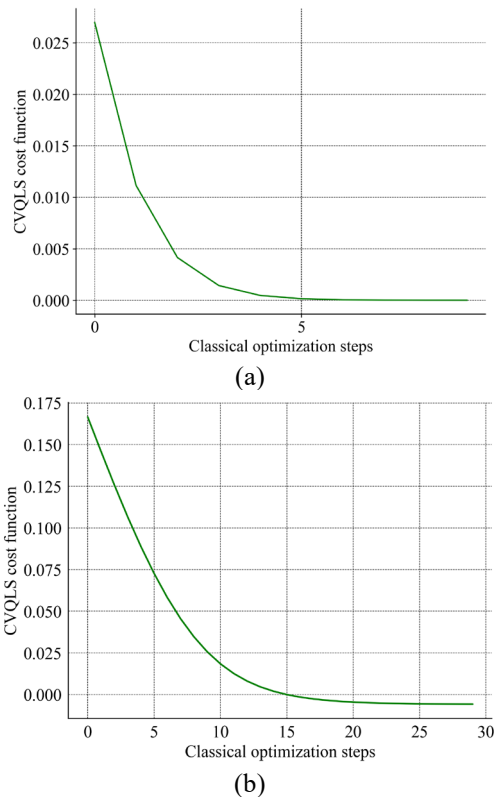


Fig. 8: CVQLS cost function for (a) ACPF matrix of 5-bus system, and (b) DCOPF of 5-bus system at 5th QIPM iteration.

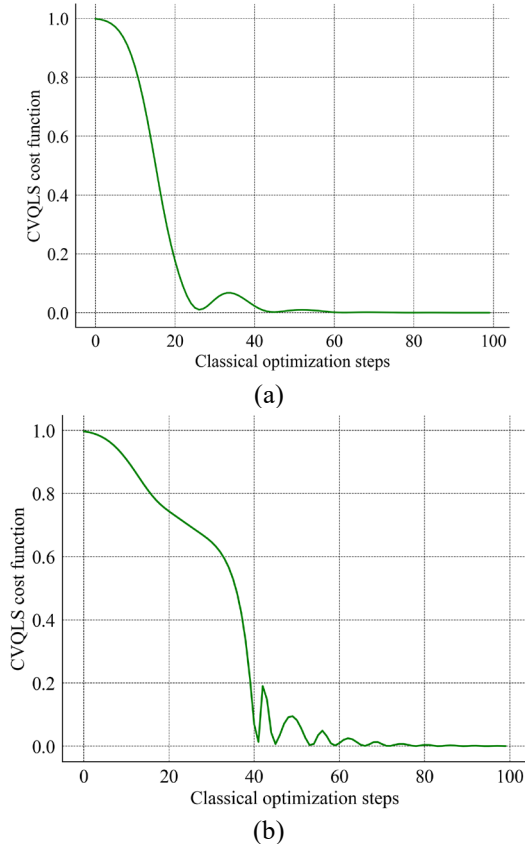


Fig. 9: CVQLS cost function of the ACOF in the 5-bus system at (a) the second QIPM iteration, and (b) the 10th iteration.

D. Q-OPF Simulation with PennyLane

We ran DCOPF and ACOF problems using Matpower with a classical IPM solver and used the results as a reference for comparing the Q-OPF outcomes with the proposed QIPM solver. CVQLS with the Adam optimizer serves as the quantum linear solver for Q-OPF. Figs. 10 and 11 illustrate that QIPM exhibits a trajectory similar to that of classical IPM. The proposed approach performs well for both the linear DCOPF and the nonlinear ACOF problems. Although ACOF is more complex due to its nonlinear nature, the approach still achieves optimal results, largely due to the implementation of the enhancement techniques discussed in Section IV. The number of QIPM iterations needed to achieve an IPM objective function value close to that of classical IPM is higher for the 5-bus system compared to the 3-bus system. This suggests that the system type and size influence the convergence trend. Increasing the number of QIPM iterations (k_{IPM}) can lead to a satisfactory solution even for the larger system. Generally, larger systems might take more iterations to provide a high-quality solution.

We note that while we tested the 3-bus and 5-bus systems on the PennyLane quantum simulator, we were unable to run larger systems due to its limited capacity for solving large systems of equations. Therefore, additional simulations are necessary to draw definitive conclusions about the QIPM effectiveness for solving larger systems, particularly for nonlinear ACOF problems. Nonetheless, with ongoing advancements in quantum simulators and hardware, we are optimistic that the proposed Q-OPF approach will be applicable to solving larger systems in the future.

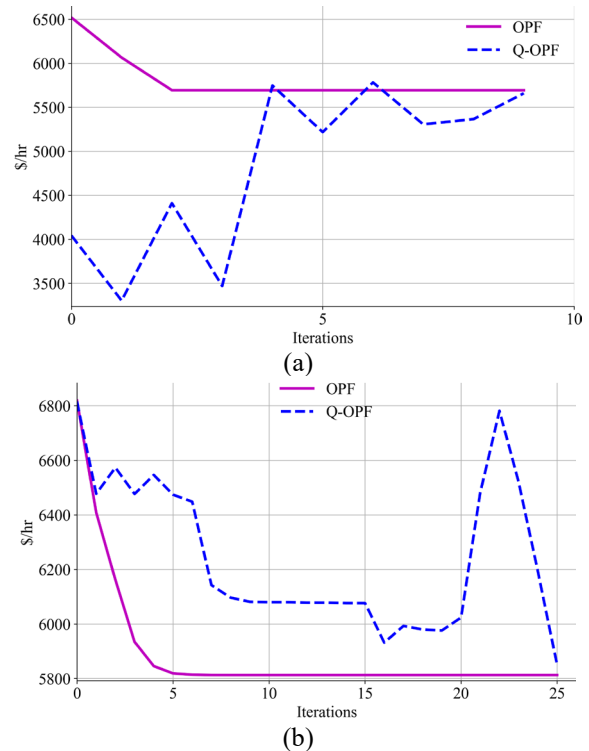


Fig. 10: Q-OPF objective function of 3-Bus system for (a) DCOPF (b) ACOF.

> REPLACE THIS LINE WITH YOUR MANUSCRIPT ID NUMBER (DOUBLE-CLICK HERE TO EDIT) <

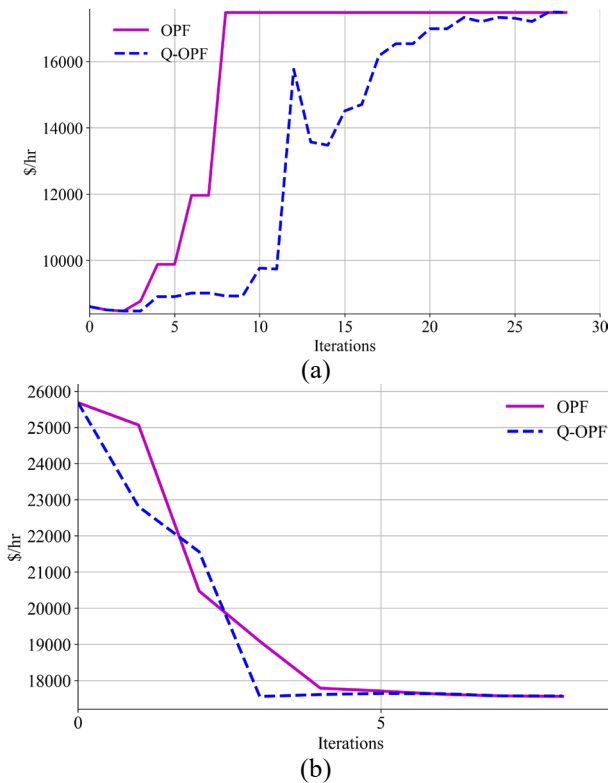


Fig. 11: Q-OPF objective function of 5-Bus system for (a) DCOPF (b) ACOPF.

E. Noise Simulation for Large Systems

To further assess the performance of the proposed approach for larger power systems, given the limitations of current quantum computing platforms, we simulate quantum computing efforts and test Q-OPF on the IEEE 118-bus and 300-bus systems. We use the Qiskit noise simulator to model errors typically encountered in real quantum computers. This simulator introduced noise into our linear system's matrix H_k and vector r_k . We still use Algorithm II to adjust μ to ensure QIPM remains stable and avoids divergence.

The DCOPF and ACOPF results for the 118-bus and 300-bus systems are shown in Figs. 12 and 13, respectively. The proposed approach performs effectively, even in the presence of errors and noise. QIPM achieves a solution that closely approximates the reference results obtained by the classical IPM. However, QIPM takes more iterations to converge, which can be attributed to the noise affecting the calculations, thereby preventing the Newton direction from rapidly converging in fewer iterations.

V. CONCLUSION

This paper presented a quantum-inspired approach for solving OPF using a variational quantum circuit, with IPM as the core optimization technique. The goal was to examine how quantum computing can be applied to power systems optimization and to tackle the challenges that arise in the process. Our comparative analysis of three quantum linear solvers—HHL, VQLS, and CVQLS—showed that CVQLS is the most suitable for OPF applications, offering more stable results than VQLS, particularly when dealing with ill-

conditioned matrices like the Hessian in IPM.

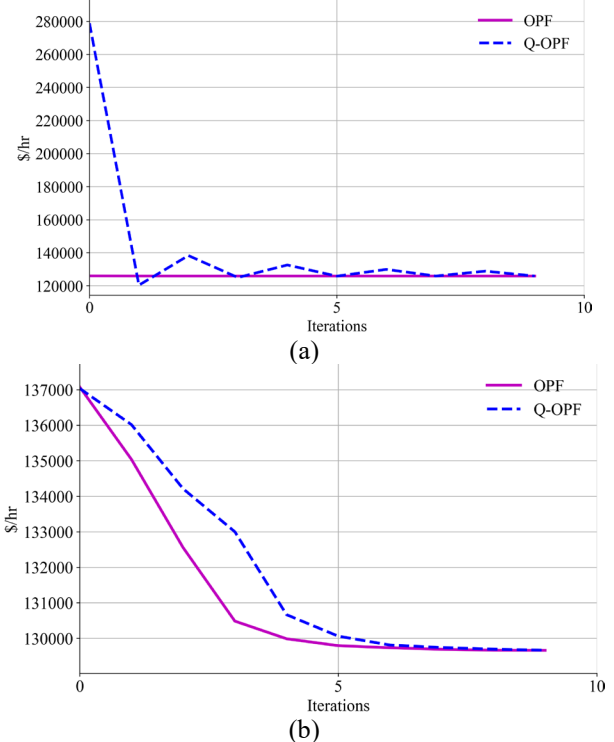


Fig. 12: Q-OPF objective function of 118-Bus system for (a) DCOPF (b) ACOPF.

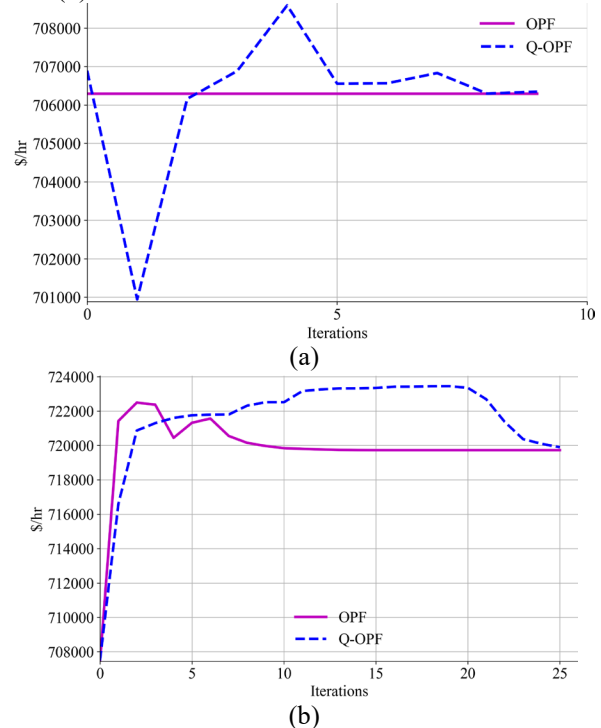


Fig. 13: Q-OPF objective function of 300-Bus system for (a) DCOPF (b) ACOPF.

We found that a shallow ansatz performed effectively, while deeper configurations struggled with overfitting and trainability, highlighting the need for careful parameter management. To improve convergence, we suggested a parameter initialization technique, using the optimal parameters from the final iteration of each IPM cycle as the starting point

> REPLACE THIS LINE WITH YOUR MANUSCRIPT ID NUMBER (DOUBLE-CLICK HERE TO EDIT) <

for the next. By using various optimizers for quantum circuit parameter optimization, we observed that CVQLS performed stable with the Adam optimizer, while VQLS exhibited instability across different optimizers. Additionally, suggested adjusting the central path parameter μ in IPM to avoid convergence to suboptimal solutions.

Although CVQLS showed promise, its application is currently limited by the capabilities of existing quantum hardware, especially for larger systems. To address this, we used a quantum noise simulator for testing on larger problems, reflecting current technological limitations. Using IPM integrated with the proposed Q-OPF, we tested the approach on IEEE 3-, 5-, 118-, and 300-bus systems, demonstrating its effectiveness in achieving satisfactory OPF solutions.

Future research should focus on enhancing the scalability of CVQLS for larger systems. Exploring advanced ansatz

design, enhanced initialization techniques, and adaptive methods for tuning classical parameters could further strengthen the robustness of Q-OPF. These efforts will help optimize the integration of quantum computing into power systems, promoting cost-effective and resilient operations under uncertainty.

REFERENCES

- [1] Z. Amiri, S. Dehdashti, K. H. El-Safty, I. Litvin, P. Munar-Vallespir, J. Nötzel, and S. Sekavčnik, "Quantum advantages for data transmission in future networks: An overview," *Computer Networks*, p. 110727, 2024.
- [2] R. Mahroo and A. Kargarian, "Learning infused quantum-classical distributed optimization technique for power generation scheduling," *IEEE Transactions on Quantum Engineering*, 2023.
- [3] C. Mastroianni, F. Plastina, J. Settino, and A. Vinci, "Variational quantum algorithms for the allocation of resources in a cloud/edge architecture," *IEEE Transactions on Quantum Engineering*, 2024.
- [4] T. Morstyn and X. Wang, "Opportunities for quantum computing within net-zero power system optimization," *Joule*, 2024.
- [5] B.-G. Risi, F. Riganti-Fulginei, and A. Laudani, "Modern techniques for the optimal power flow problem: State of the art," *Energies*, vol. 15, no. 17, p. 6387, 2022.
- [6] F. Hasan, A. Kargarian, and J. Mohammadi, "Hybrid learning aided inactive constraints filtering algorithm to enhance ac opf solution time," *IEEE Transactions on Industry Applications*, vol. 57, no. 2, pp. 1325–1334, 2021.
- [7] T. Morstyn, "Annealing-based quantum computing for combinatorial optimal power flow," *IEEE Transactions on Smart Grid*, vol. 14, no. 2, pp. 1093–1102, 2022.
- [8] J. Zhu, X. Mo, Y. Xia, Y. Guo, J. Chen, and M. Liu, "Fully-decentralized optimal power flow of multi-area power systems based on parallel dual dynamic programming," *IEEE Transactions on Power Systems*, vol. 37, no. 2, pp. 927–941, 2021.
- [9] H. Alhakami, "Enhancing iot security: Quantum-level resilience against threats," *Computers, Materials & Continua*, vol. 78, no. 1, 2024.
- [10] J. van den Brand, "A deterministic linear program solver in current matrix multiplication time," in *Proceedings of the Fourteenth Annual ACM-SIAM Symposium on Discrete Algorithms*. SIAM, 2020, pp. 259–278.
- [11] S. Akram and Q. U. Ann, "Newton raphson method," *International Journal of Scientific & Engineering Research*, vol. 6, no. 7, pp. 1748–1752, 2015.
- [12] J. V. Frasch, S. Sager, and M. Diehl, "A parallel quadratic programming method for dynamic optimization problems," *Mathematical programming computation*, vol. 7, pp. 289–329, 2015.
- [13] J. D. Kelleher, *Deep learning*. MIT press, 2019.
- [14] D. Tiwari, M. J. Zideh, V. Talreja, V. Verma, S. K. Solanki, and J. Solanki, "Power flow analysis using deep neural networks in three-phase unbalanced smart distribution grids," *IEEE Access*, 2024.
- [15] J. Gondzio, "Interior point methods 25 years later," *European Journal of Operational Research*, vol. 218, no. 3, pp. 587–601, 2012.
- [16] F. A. Potra and S. J. Wright, "Interior-point methods," *Journal of computational and applied mathematics*, vol. 124, no. 1-2, pp. 281–302, 2000.
- [17] Y. Ye, *Interior point algorithms: theory and analysis*. John Wiley & Sons, 2011.
- [18] H. Kou, Y. Zhang, and H. P. Lee, "Dynamic optimization based on quantum computation—a comprehensive review," *Computers & Structures*, vol. 292, p. 107255, 2024.
- [19] A. W. Harrow, A. Hassidim, and S. Lloyd, "Quantum algorithm for linear systems of equations," *Physical review letters*, vol. 103, no. 15, p. 150502, 2009.
- [20] C. Bravo-Prieto, R. LaRose, M. Cerezo, Y. Subasi, L. Cincio, and P. J. Coles, "Variational quantum linear solver," *Quantum*, vol. 7, p. 1188, 2023.
- [21] H.-Y. Huang, R. Kueng, and J. Preskill, "Information-theoretic bounds on quantum advantage in machine learning," *Physical Review Letters*, vol. 126, no. 19, p. 190505, 2021.
- [22] F. Amani and A. Kargarian, "Quantum-inspired optimal power flow," in *2024 IEEE Texas Power and Energy Conference (TPEC)*. IEEE, 2024, pp. 1–6.
- [23] A. Zaman and H. Y. Wong, "Study of error propagation and generation in harrow-hassidim-lloyd (hhl) quantum algorithm," in *2022 IEEE Latin American Electron Devices Conference (LAEDC)*. IEEE, 2022, pp. 1–4.
- [24] K. Bharti, A. Cervera-Lierta, T. H. Kyaw, T. Haug, S. Alperin-Lea, A. Anand, M. Degroote, H. Heimonen, J. S. Kottmann, T. Menke et al., "Noisy intermediate-scale quantum algorithms," *Reviews of Modern Physics*, vol. 94, no. 1, p. 015004, 2022.
- [25] M. Cerezo, A. Arrasmith, R. Babbush, S. C. Benjamin, S. Endo, K. Fujii, J. R. McClean, K. Mitarai, X. Yuan, L. Cincio et al., "Variational quantum algorithms," *Nature Reviews Physics*, vol. 3, no. 9, pp. 625–644, 2021.
- [26] A. Choquette, A. Di Paolo, P. K. Barkoutsos, D. Sénéchal, I. Tavernelli, and A. Blais, "Quantum-optimal-control-inspired ansatz for variational quantum algorithms," *Physical Review Research*, vol. 3, no. 2, p. 023092, 2021.
- [27] S. Halder, A. Dey, C. Shrikhande, and R. Maitra, "Machine learning assisted construction of a shallow depth dynamic ansatz for noisy quantum hardware," *Chemical Science*, vol. 15, no. 9, pp. 3279–3289, 2024.
- [28] M. Telahun, "Exploring information for quantum machine learning models," 2020.
- [29] C. J. Trahan, M. Loveland, N. Davis, and E. Ellison, "A variational quantum linear solver application to discrete finite-element methods," *Entropy*, vol. 25, no. 4, p. 580, 2023.
- [30] F. Feng, Y.-F. Zhou, and P. Zhang, "Noise-resilient quantum power flow," *iEnergy*, vol. 2, no. 1, pp. 63–70, 2023.
- [31] F. Amani, R. Mahroo, and A. Kargarian, "Quantum-enhanced DC optimal power flow," in *2023 IEEE Texas Power and Energy Conference (TPEC)*. IEEE, 2023, pp. 1–6.
- [32] X. Gao and L.-M. Duan, "Efficient representation of quantum manybody states with deep neural networks," *Nature communications*, vol. 8, no. 1, p. 662, 2017.
- [33] J. R. McClean, M. E. Kimchi-Schwartz, J. Carter, and W. A. De Jong, "Hybrid quantum-classical hierarchy for mitigation of decoherence and determination of excited states," *Physical Review A*, vol. 95, no. 4, p. 042308, 2017.
- [34] M. Cerezo, A. Sone, T. Volkoff, L. Cincio, and P. J. Coles, "Cost function dependent barren plateaus in shallow parametrized quantum circuits," *Nature communications*, vol. 12, no. 1, p. 1791, 2021.
- [35] A. K. Khamees, N. Badra, and A. Y. Abdelaziz, "Optimal power flow methods: A comprehensive survey," *International Electrical Engineering Journal (IEEJ)*, vol. 7, no. 4, pp. 2228–2239, 2016.
- [36] S. Park, W. Chen, T. W. Mak, and P. Van Hentenryck, "Compact optimization learning for ac optimal power flow," *IEEE Transactions on Power Systems*, 2023.
- [37] Y. Shee, P.-K. Tsai, C.-L. Hong, H.-C. Cheng, and H.-S. Goan, "Qubit-efficient encoding scheme for quantum simulations of electronic structure," *Physical Review Research*, vol. 4, no. 2, p. 023154, 2022.
- [38] M. Kjaergaard, M. Schwartz, A. Greene, G. Samach, A. Bengtsson, M. O’Keeffe, C. McNally, J. Braumüller, D. Kim, P. Krantz et al., "Demonstration of density matrix exponentiation using a superconducting quantum processor," *Physical Review X*, vol. 12, no. 1, p. 011005, 2022.
- [39] M. Weigold, J. Barzen, F. Leymann, and M. Salm, "Data encoding patterns for quantum computing," in *Proceedings of the 27th Conference on Pattern Languages of Programs*, 2020, pp. 1–11.

> REPLACE THIS LINE WITH YOUR MANUSCRIPT ID NUMBER (DOUBLE-CLICK HERE TO EDIT) <

- [40] R. M. N. Pesce and P. D. Stevenson, "H2zixy: Pauli spin matrix decomposition of real symmetric matrices," *arXiv preprint arXiv:2111.00627*, 2021.
- [41] L. Hantzko, L. Binkowski, and S. Gupta, "Tensorized pauli decomposition algorithm," *Physica Scripta*, vol. 99, no. 8, p. 085128, 2024.
- [42] M. Kashif, M. Rashid, S. Al-Kuwari, and M. Shafique, "Alleviating barren plateaus in parameterized quantum machine learning circuits: Investigating advanced parameter initialization strategies," in *2024 Design, Automation & Test in Europe Conference & Exhibition (DATE). IEEE*, 2024, pp. 1–6.
- [43] X. Liu, G. Liu, H.-K. Zhang, J. Huang, and X. Wang, "Mitigating barren plateaus of variational quantum eigensolvers," *IEEE Transactions on Quantum Engineering*, 2024.
- [44] J. R. McClean, S. Boixo, V. N. Smelyanskiy, R. Babbush, and H. Neven, "Barren plateaus in quantum neural network training landscapes," *Nature communications*, vol. 9, no. 1, p. 4812, 2018.
- [45] A. Skolik, J. R. McClean, M. Mohseni, P. Van Der Smagt, and M. Leib, "Layerwise learning for quantum neural networks," *Quantum Machine Intelligence*, vol. 3, pp. 1–11, 2021.
- [46] E. Grant, L. Wossnig, M. Ostaszewski, and M. Benedetti, "An initialization strategy for addressing barren plateaus in parametrized quantum circuits," *Quantum*, vol. 3, p. 214, 2019.
- [47] R. Sweke, F. Wilde, J. Meyer, M. Schuld, P. K. Fährmann, B. Meynard-Piganeau, and J. Eisert, "Stochastic gradient descent for hybrid quantum-classical optimization," *Quantum*, vol. 4, p. 314, 2020.
- [48] M. Colombo, "Advances in interior point methods for large-scale linear programming," 2007.
- [49] A. Domahidi, A. U. Zraggen, M. N. Zeilinger, M. Morari, and C. N. Jones, "Efficient interior point methods for multistage problems arising in receding horizon control," in *2012 IEEE 51st IEEE conference on decision and control (CDC)*. IEEE, 2012, pp. 668–674.



FARSHAD AMANI-JOUNEGHANI

(Student Member, IEEE) received his B.Sc. degree in Electrical Engineering from the Iran University of Science and Technology, Tehran, Iran, in 2017, and his M.Sc. degree in Power Systems Engineering from the Sharif University of Technology, Tehran, Iran, in 2020. He has been pursuing a Ph.D. in Electrical

Engineering at Louisiana State University, Baton Rouge, LA, USA, since 2022.

His research interests include optimization, quantum computing, quantum optimization, machine learning, smart grids, power system reliability and resilience, and the operation and planning of power distribution systems.



Amin Kargarian (Senior Member, IEEE) received the M.Sc. degree from Shiraz University, Iran, 2010 and the Ph.D. in electrical and computer engineering from Mississippi State University, Starkville, MS, USA, in 2014. From 2014 to 2015, he was a Postdoctoral Research Associate with

the Department of Electrical and Computer Engineering, Carnegie Mellon University, Pittsburgh, PA, USA. He is currently an Associate Professor with the Electrical and Computer Engineering Department, at Louisiana State University, Baton Rouge, LA, USA.

His research interests include optimization, machine learning, quantum computing, and their applications to power systems.